ELSEVIER

Contents lists available at SciVerse ScienceDirect

## Thin Solid Films

journal homepage: www.elsevier.com/locate/tsf



# Spinodal decomposition of Ti<sub>0.33</sub>Al<sub>0.67</sub>N thin films studied by atom probe tomography

L.J.S. Johnson a,\*, M. Thuvander b, K. Stiller b, M. Odén a, L. Hultman a

- <sup>a</sup> Dept. of Physics, Chemistry and Biology (IFM), Linköping University, SE-581 83, Sweden
- <sup>b</sup> Dept. of Applied Physics, Chalmers University of Technology, SE-421 96, Sweden

#### ARTICLE INFO

Article history:
Received 22 September 2011
Received in revised form 15 February 2012
Accepted 23 February 2012
Available online 3 March 2012

Keywords: Titanium aluminum nitride Spinodal decomposition Atom probe tomography Thin films

#### ABSTRACT

Details of the phase decomposition in NaCl-structure Ti<sub>0.33</sub>Al<sub>0.67</sub>N thin films deposited by cathodic arc evaporation are studied by atom probe tomography. We demonstrate that as-deposited films are in the earliest stage of decomposition for which electron microscopy and x-ray diffraction indicate a single-phase solid solution. Annealing at 900 °C further activates spinodal decomposition of the films, although pockets of undecomposed material remain after 2 h. N preferentially segregates to the AlN and TiN domains, causing the TiAlN matrix to be understoichiometric, by the energetics of N vacancies in TiAlN. The corresponding modulation in stoichiometry implies a Kirkendall effect, caused by different Al and Ti diffusivities.

© 2012 Elsevier B.V. All rights reserved.

#### 1. Introduction

TiAlN thin films are used extensively as cutting tool coatings. They exhibit age hardening as described by Hörling et al. [1,2], who also showed that the effect is caused by the decomposition of metastable cubic B1-TiAlN upon heating, such as during cutting operations. The decomposition proceeds in two steps. Firstly, Ti and Al segregates to form c-TiN and metastable c-AlN coherently strained domains, where c-AlN is stabilized by coherency forces in the first step of separation. Secondly, the c-AlN transforms, upon further annealing, into h-AlN, which is the thermodynamically stable phase of AlN at ambient pressure [3]. The apparent segregation of Ti and Al on the cubic lattice is due to the existence of a miscibility gap in the pseudobinary TiN-AlN system [2,4]. This, and a number of observations [2,5–9], point to a spinodal decomposition mechanism.

The difficulty of proving the hypothesis of the operation of spinodal decomposition in the TiAlN thin film material system stems from the fact that it proceeds at very small size scales and high temperatures, for which traditional thin film microstructural characterization techniques are insufficient and results inconclusive. This situation is changing with technological progress in instrumentation. Of particular interest for this kind of problem is atom probe tomography (APT), which has the power to resolve the composition of a sample with high accuracy at high resolution [10]. Recent advances [11,12], such as the laser assisted field evaporation, local counterelectrodes and focussed ion beam (FIB) specimen preparation techniques, allow the analysis of thin films of nonconductive materials. Rachbauer et al.

[8,13] studied the separation of magnetron sputtered Ti<sub>0.5</sub>Al<sub>0.5</sub>N films by APT adding to the evidence for spinodal decomposition in the system. A more detailed description of the evolving compositional variations during the spinodal process is lacking, and furthermore, very little is known about the behavior of N during the decomposition and its influence on the same.

Here, we use APT to investigate the decomposition of  ${\rm Ti_{0.33}Al_{0.67}N}$  thin films deposited by reactive cathodic arc evaporation. The choice of this high Al content is motivated by the facts that such a composition is typical for industrial coatings and that the system is close to the center of the miscibility gap [4,14]. We discuss the separation of Ti and Al as well as the coupled changes in N stoichiometry.

#### 2. Experimental details

The films were deposited by reactive cathodic arc evaporation in a Metaplas MXR323 system with samples fixtured to a rotating drum. The substrates were polished cemented carbide (WC-Co, Seco Tools "HX") flat inserts of dimensions  $13 \times 13 \times 4$  mm. Prior to deposition the substrates were sputter cleaned with Ar ions. During the deposition the atmosphere was pure (99.995%) N<sub>2</sub>, the substrate temperature was ~400 °C and a bias of  $-55\,\text{V}$  was applied. The resulting films were of a B1 NaCl structure with a lattice parameter of 4.15 Å as determined by X-ray diffraction (XRD), with a total thickness of ~3 \mum. Rutherford backscattering spectroscopy (RBS) gave the mean composition of the films as (Ti<sub>0.33</sub>Al<sub>0.67</sub>)N<sub>0.92</sub>, with O contamination on the level of 0.5–1 at.%. The microstructure was found to be of a dense columnar type [5].

Isothermal annealing of a sample was performed for 120 min at 900 °C in an inert argon atmosphere with a Sintervac furnace (GCA Vacuum Industries). The heat treatment parameters were chosen

<sup>\*</sup> Corresponding author. Tel.: +46 13 282907. E-mail address: larsj@ifm.liu.se (L.J.S. Johnson).

according to the results of Hörling et al. [5] to produce as much c-AlN as possible before transformation to the stable h-AlN occurs.

Samples for APT were prepared using the FIB lift-out technique [15] where wedges roughly 3  $\mu$ m high and 1–2  $\mu$ m wide are attached to posts fabricated out of a silicon wafer. The wedges were sharpened by annular milling at 30 keV and – for the last stage – 5 keV Ga<sup>+</sup> ions.

The samples were analyzed in a local electrode atom probe (Imago LEAP 3000X HR) in laser pulsing mode with a pulse rate of 200 kHz, a pulse energy of 0.35 nJ, and a target evaporation rate of 0.5% (expressed as detected ions per pulse) at 65 K. The laser energy was chosen after trials to provide the optimum mass resolution. Four tips from the as-deposited state and six from the annealed state were analyzed. For reconstruction, an evaporation field of 40 V/nm, image compression factor of 1.65 and a field factor of 3.3 were used, which gave final tip radii close to or in agreement with measurements by scanning electron microscopy on the tips after evaporation.

#### 3. Data analysis

For the application of APT to the problem of spinodal decomposition Miller et al. [16–18] is the most recent general treatment.

The main variable of interest for spinodal decomposition is the mole fraction describing the separation:

$$x = n_{Al}/(n_{Al} + n_{Ti}), \tag{1}$$

where n is the concentration of a species. For transition metal nitrides the stoichiometry of N may have a large effect on the properties of the alloy [19–21]; we take it as:

$$z = n_N/(n_N + n_{Al} + n_{Ti}) \approx n_N, \tag{2}$$

effectively giving  $(Ti_{1-x}AI_x)_{1-z}N_z$ . The two variables were computed on a regular grid of  $1 \text{ nm}^3$  cubes by first binning all detected ions using Gaussian delocalization with the IVAS software, and then computing the field variables for each voxel.

The autocorrelation functions of the field variables were computed to investigate any spatial correlations present in the data. The autocorrelation function,  $\gamma(r)$ , for variable x was computed as:

$$\gamma(\vec{r}) = \frac{1}{\sigma_x^2(N-1)} \sum_{\vec{r}'} (x_{\vec{r}'} - \bar{x})(x_{\vec{r}' - \vec{r}} - \bar{x}), \tag{3}$$

where  $\bar{x}$  is the mean,  $\sigma_x$  the standard deviation, N the number of voxels, and  $\bar{r}'$  ranges over all valid voxel indices in the datacube. The function was then averaged radially by integration using cylindrical coordinates:

$$\gamma(r,z) = \frac{1}{2\pi} \int_{0}^{2\pi} \gamma(r\cos(\phi), r\sin(\phi), z) d\phi. \tag{4}$$

Radial distribution functions (RDF) are another way to show spatial correlations. In the case that a strong spatial variation in one variable influences the one for which a RDF is sought, the RDF may be extended by taking the variation of the first variable into account and binning the RDF: let  $g^i{}_a(r)$  be the RDF of variable a for atom i and  $g^i{}_a$  its average up to the radius  $r_0$ :

$$g_a^i(r) = g_a^i(r)_r, r \in [0, r_0].$$
 (5)

Then the binned RDF of variable b is:

$$g_h(r,a) = g_h^i(r)_i, \forall i : g_a^i \in [a - \Delta a, a + \Delta a]. \tag{6}$$

The field variables of interest are sensitive to the sampling nature of the technique, as the collection efficiency is less than one (0.37 for

the instrument used in this study). Danoix et al. [22] analyzed this situation in detail for the case of a two-component system. They showed that the variance of the measured atomic composition, *c*, of a box is:

$$\sigma_c^2 = p_0(1 - p_0)(1 - \eta)/n,\tag{7}$$

where  $p_0$  is the true composition,  $\eta$  is the detection efficiency, and n is the mean number of ions per box (atomic density per box, m, times the efficiency), for reasonable detection efficiencies and box sizes ( $m \ge 100$ ).

In order to test the hypothesis that a sample is homogeneous, an empirical test distribution was created by simulating the model described above. A sample was considered to consist of 40 000 sample cubes (1 nm³ in volume) of a B1 structure of appropriate density, the variance of the composition variable was calculated for each sample. Two thousand (2000) simulations were performed, and the distribution of variances was calculated, giving a p-value resolution of 0.0005. This allowed the testing of the measured variance of the composition of samples against the null hypothesis that the observed variance could be explained by the variance inherent in the measurement, by directly calculating the probability that the observed variance was in accordance with the null hypothesis.

#### 4. Results

#### 4.1. Mass spectra and evaporation behavior

A typical mass spectrum from a  $Ti_{0.33}Al_{0.67}N$  film is shown in Fig. 1, and the corresponding charge state ratios are given in Table 1. Ions of Ti (doubly and triply charged), Al (singly to triply charged), and N (singly and doubly charged) are present. Of note is the large amount of complex ions, where  $TiN^{2+}$  is the dominating complex, but  $AlN^{2+}$  and  $AlO^{2+}$  are present as well. No peaks corresponding to either O or TiO complexes were observed. Tied to the high number of complexes were a corresponding amount of multiple evaporation events per laser pulse. Finally, although the  $Al^{2+}$  and  $N^{+}$  peaks are well separated, the tail of the  $Al^{2+}$  peak overlaps with the  $N^{+}$  peak to a significant degree, most probably due to the limited thermal conductance of the film. This slows down the cooling of the APT tip after heating by each laser pulse, which increases the time window for evaporation, which in turn leads to the broadening of the peak tails.

The composition of the samples, obtained by peak decomposition using natural isotope abundances and statistical averaging, is shown in Table 2. This method uses the whole spectrum, and as such it is not applicable to the ranging of ions for the volume reconstruction, which will be worse at resolving the overlap of the  $Al^{2+}$  and  $N^{+}$  peaks (compare with Fig. 3). The metal pseudobinary ratio, x, in  $Ti_{1-x}Al_xN$ , is close to 0.6 for both samples. This is below the expected 0.67 value as confirmed by RBS measurements. This

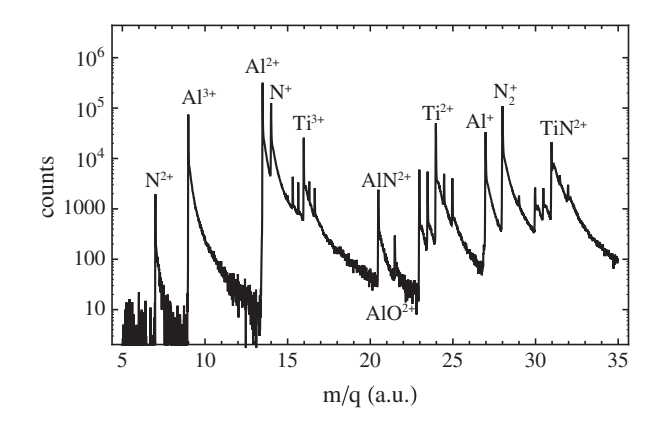


Fig. 1. Laser atom probe mass spectrum from Ti<sub>0.33</sub>Al<sub>0.67</sub>N.

### Download English Version:

# https://daneshyari.com/en/article/1667475

Download Persian Version:

https://daneshyari.com/article/1667475

Daneshyari.com